JOURNAL OF MATERIALS SCIENCE **39** (2004) 335–338

Fatigue strength variation by crack initiation origin of surface hardened Cr-Mo steel alloy

SAM-HONG SONG
Department of Mechanical Engineering, College of Engineering, Korea University, Seoul 136-701, Republic of Korea

BYOUNG-HO CHOI
Department of Civil and Material Engineering, University of Illinois at Chicago, Chicago, IL 60607, USA
E-mail: cgbiho@uic.edu

It is very difficult to predict the fatigue strength of a surface hardened specimen due to external factors such as residual stress, hardness distribution, and inclusions, which are major reasons for the initiation of internal fatigue crack. Even though many researchers [1–3] have reported experimental fatigue behavior on the surface hardened specimen, the analysis based on fracture mechanics for the fatigue strength variation is still insufficient. Fatigue strength variation due to internal origin of a fracture from inclusions, called fish-eye fracture, is very important in determining the fatigue limit of a high strength and a surface hardened steel [4, 5]. Therefore, investigation of the size and position of an inclusion, which is the origin of a fracture, will provide meaningful clues for the determination of the fatigue limit and the fatigue strength. Murakami *et al*. [6] suggested $\sqrt{\text{area}}$ as a fracture mechanics parameter, while Song and Choi [7] proposed a modified relationship using the parameter for the prediction of a fatigue limit of a hardened steel with defects on the surface. In this paper, the distribution of inclusions, which are the origins of fish-eye fracture is examined experimentally. The evaluation of the fatigue strength for the induction surface hardened steel is also considered using the relation proposed by Song and Choi [7]. If the statistical distribution of the inclusion inside the surface hardened steel can be determined, the quantitative fatigue limit prediction of the surface hardened steel will be possible using the results of this paper.

Cr-Mo steel alloy (C: 0.41%, Si: 0.25%, Mn: 0.68%, Cr: 1.05%, Mo: 0.23%), defined as SCM440 in Korea Standard, was used. The materials were annealed at 850 °C for one hour, and the specimens were machined for rotary bending fatigue tests. Three different hardening depths were applied using induction surface

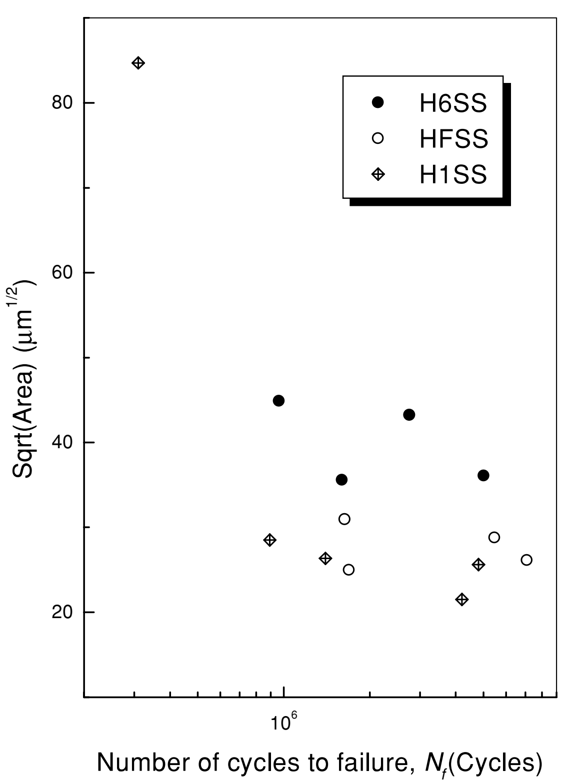

Figure 1 Relationship between number of cycles to failure and $\sqrt{\text{area}}$.

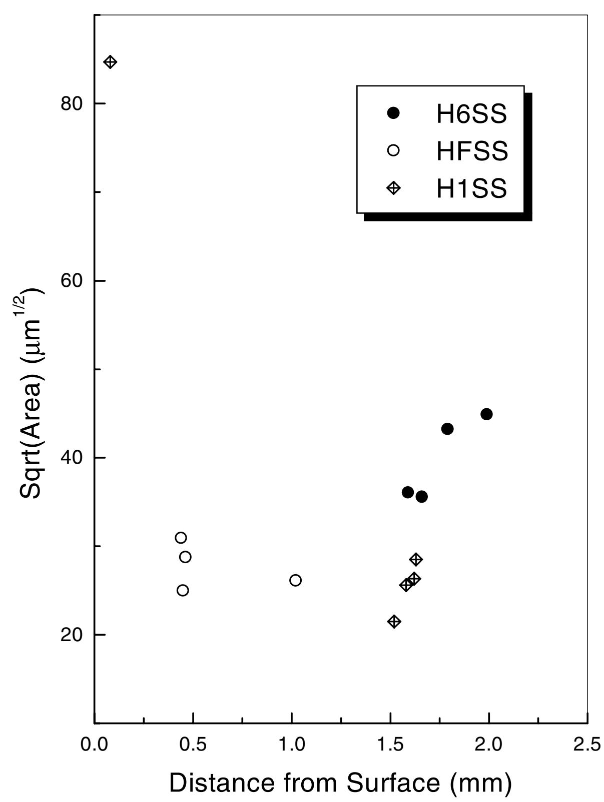

Figure 2 Relationship between distance from surface and $\sqrt{\text{area}}$.

TABLE I Residual stress and microvickers hardness obtained by experiment

	HFSS	H1SS	H6SS
Surface hardness (HV)	560	560	560
Maximum hardness (HV)	575	570	570
Effective case depth (mm)	–	1.1	1.6
Full case depth (mm)	4.5	2.0	2.4
Hardening ratio	1	0.24	0.35
Residual stress at surface (MPa)	−322.8	−451.1	−383.4
Maximum residual stress (MPa)	−416.9	−596.6	−434.6

hardening and the hardening conditions are shown in Table I. The test machine was an Ono-type rotary bending fatigue tester which can give 98 N-m of maximum bending moment, the rotation speed was 3000 rpm and the applied stress ratio (R) was -1.

In Fig. 1, the relation between the projected area for 3-D inclusion ($\sqrt{\text{area}}$) and the fractured lifetime is shown. Even though there is a large scatter in the figure, it can be seen that in general the projected size of observed inclusion becomes smaller as the fractured lifetime becomes longer. It means that a small inclusion can be an origin of a fatigue crack close to the fatigue limit.

In Fig. 2, the relation between $\sqrt{\text{area}}$ and the position of observed crack origin is presented. The positions of the crack origin of HF specimen are much closer to the specimen surface than those of H1 and H6 specimens. It is caused by the distribution of compressive residual stress and the hardness of each specimen [8]. Moreover, the inclusion positions of H6 specimen are deeper than those of H1 specimen and are close to full case depth, which is also caused by the combination

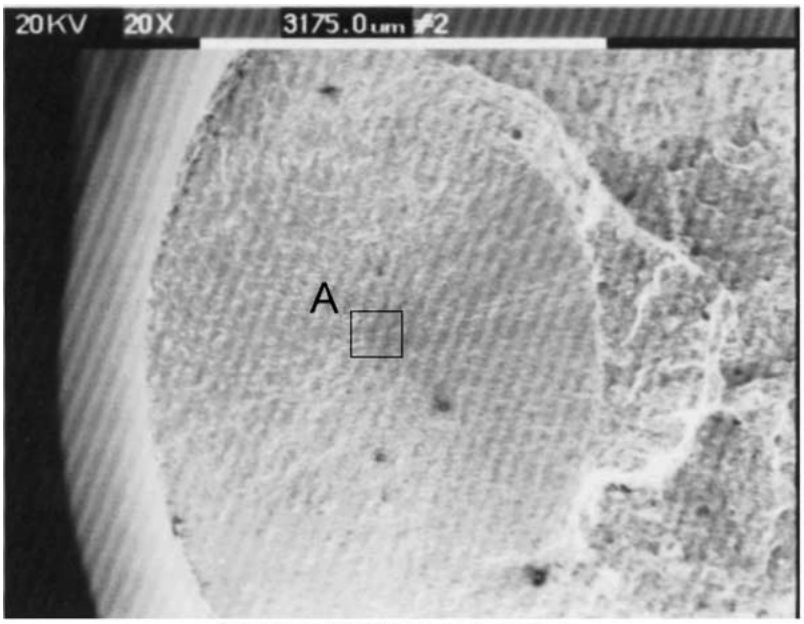

(a) Photo for fractured surface

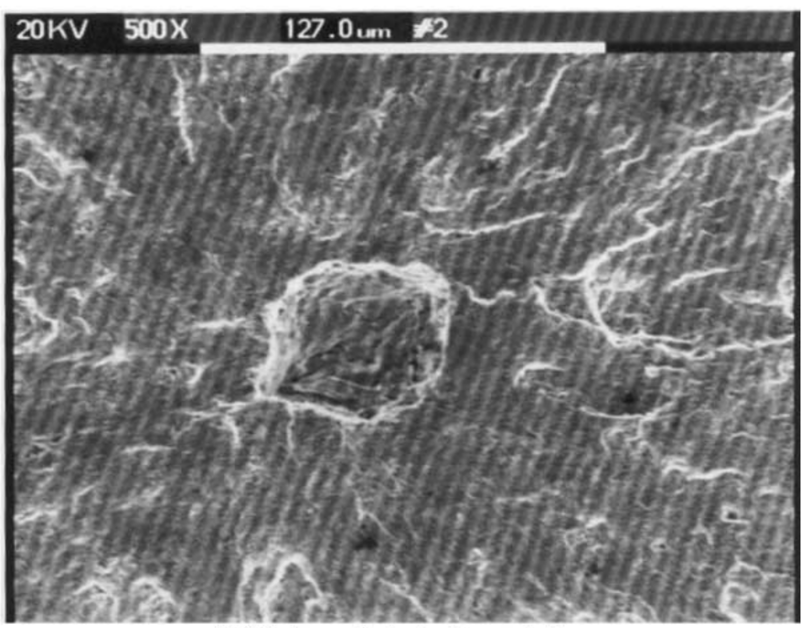

(b) Enlarged photo for part A

Figure 3 Fractographies of fish-eye fracture (H6SS: $N_f = 5.01 \times 10^{-6}$ cycles).

TABLE II Results of fatigue limit prediction of inner defects

Specimen	Failure cycle: Depth (mm)	N_f (cycles)	$\sqrt{\text{area}}$ (μm)	Nominal stress, σ'_{exp} (MPa)	Predicted fatigue limit, $\sigma'_{w,pre}$	Normalized ratio, $\sigma'_{exp}/\sigma'_{w,pre}$
H6SS	1.66	1.60×10^6	35.61	466	424	1.099
	1.99	9.63×10^5	44.92	418	352	1.187
	1.79	2.75×10^6	43.24	470	401	1.172
	1.59	5.01×10^6	36.09	480	463	1.036
H1SS	1.62	1.40×10^6	24.34	497	425	1.169
	1.58	8.94×10^5	25.62	515	456	1.129
	1.63	4.80×10^6	28.50	502	420	1.195
	1.52	4.20×10^6	21.50	488	485	1.006
	0.08	3.10×10^5	84.70	707	721	0.981
HFSS	1.02	7.09×10^6	26.15	734	758	0.968
	0.44	1.63×10^6	30.94	902	792	1.139
	0.448	1.69×10^6	24.99	922	862	1.069
	0.46	5.46×10^6	28.80	866	851	1.018

of the hardness and the residual stress distribution. So, the dangerous area for each specimen can be classified from the experimental results. In Fig. 3, an example of observed fish-eye fracture surface and the origin for H6SS specimen are shown.

It is well known that the two-step S-N diagram for high strength steel and surface hardened steel is caused by inclusions or defects inside the steel. So, the prediction of fatigue strength for fish-eye fracture can be useful for the prediction of the fatigue limit.

Murakami [9] proposed the following threshold stress intensity factor for internal inclusion.

$$\Delta K_{th} = \sigma'_w \sqrt{\pi \sqrt{\text{area}}} \tag{1}$$

where σ'_w is fatigue strength. Based on Murakami's equation, Song and Choi suggested the empirically-modified fatigue limit prediction for the artificial surface defect for hardened steel [7]. In the same way of analysis, comparing the Equation 1 and the experimental relationship of threshold stress intensity factor for the surface hardened steel, the following relation for the fatigue strength can be obtained.

$$\sigma'_w = \frac{1.89(HV + 120)}{(\kappa\sqrt{\text{area}})^{1/6}} \tag{2}$$

where HV is the microvickers hardness at the position of inclusion and κ is modified coefficient considering the stationary crack. Because the value of κ for the fish-eye fracture initiation is very hard to define by experiment, κ obtained from surface-defect specimen [7] is used in the paper. Using the modified stress ratio, R_{mod}, Equation 2 can be rewritten.

$$\sigma'_w = \frac{1.89(HV + 120)}{(\kappa\sqrt{\text{area}})^{1/6}} \cdot \left(\frac{1 - R_{mod}}{2}\right) \tag{3}$$

where $R_{mod} = (\sigma_{min} + m\sigma_r)/(\sigma_{max} + m\sigma_r)$ and material coefficient for residual stress relaxation effect, m, is 0.506 [7].

By applying Equation 3 to inclusions observed in fractured specimens, the applicability of the proposed equation is examined. The residual stress and the microvickers hardness are the values at the position of the inclusion. In addition, because the calculated result from Equation 3 is not surface stress but nominal stress at the position of inclusion (σ'_{exp}), the prediction results should also be compared with the nominal stress calculated considering the applied stress and residual stress. So, if the normalized nominal stress ratio, $\sigma'_{exp}/\sigma'_{w,pre}$, exceeds 1, it means the crack can initiate at the point.

In Table II, the predicted results of fatigue limit of inner defects are presented. In Fig. 4, modified *S-N* diagram using by Equation 3 is shown. If fractured lifetime becomes longer, knowing from the Fig. 4, the normalized ratio, $\sigma'_{exp}/\sigma_{w,pre}$, is roughly close to 1. This is because the fatigue strength for each inclusion is

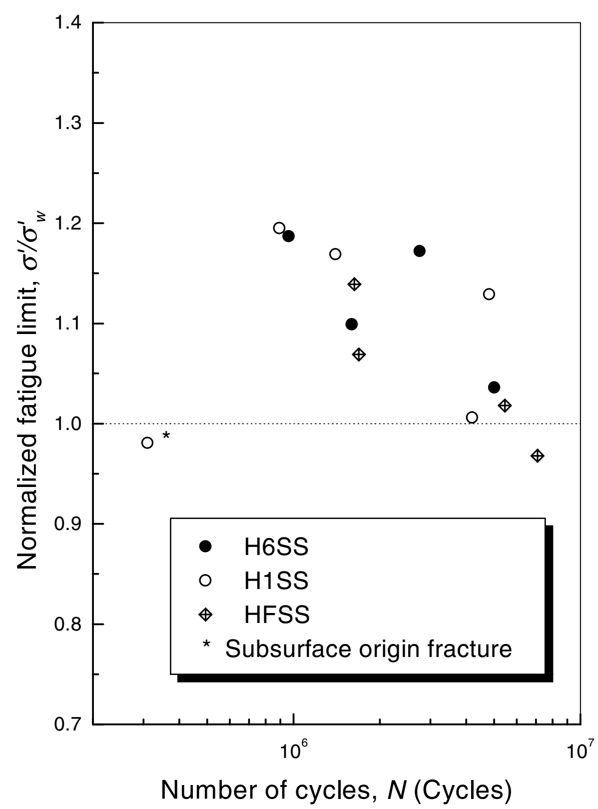

Figure 4 Modified S-N diagram by Equation 3.

close to fatigue limit of the specimen. Recently, some researchers have reported unexpected failure of a high strength or a surface hardened steel with very high lifetime [10]. So, the statistical distribution of actual inclusion should be addressed for accurate fatigue limit prediction for the surface hardened steel. However, because the normalized nominal stress ratio is already close to 1 at 10^7 cycles, the variation of the normalized stress ratio for longer failure cycles will not be so large.

Based on the experimental results and the discussions, the conclusion of this paper is the following. First, the projected size of the fracture initiating inclusion becomes smaller as the fractured lifetime becomes longer. The position of the inclusion varies with case depth. Second, by applying a modified fatigue strength prediction equation, the normalized fatigue strength ratio is close to 1, which implies the fatigue strength for each inclusion is close to the fatigue limit of the specimen.

References

1. T. FURUKAWA, *et al.*, *ISIJ* **72**(1) (1986) 62.
2. T. FURUKAWA, *et al.*, *J. Soc. Mater, Sci. Jpn.* **37**(413) (1988) 178.
3. S. H. SONG, S. H. LEE and S. H. IM, *KSPE Journal* **14**(5) (1997) 128.
4. T. ABE and K. KANAZAWA, *J. Soc. Mater. Sci. Jpn.* **40**(458) (1991) 1447.
5. Y. KUROSHIMA, M. SHIMIZU and I. KAWASAKI, *Trans. JSME* A **56**(529) (1990) 1920.
6. Y. MURAKAMI and M. ENDO, *Eng. Frac. Mech.* **11**(1) (1983) 1.
7. S.-H. SONG and B.-H. CHOI, *Mater. Sci. Eng.* A (2003) accepted to publication.
8. *Idem.*, in Proc. of Fatigue 99, Beijing, June 1999, edited by X. R. Wu (EMAS, 1999) p. 595.
9. Y. MURAKAMI, S. KODAMA and S. KONUMA, *Int. J. Fatigue* **11**(5) (1989) 291.
10. T. SAKAI, *et al.*, in Proc. of Int. Conf. 2001: Fatigue in Very High Cycle Region (2001) p. 51

Received 25 March
and accepted 18 July 2003